ATL-PHYS-2002-024
11 October 2002

Top-Antitop spin correlation measurement in the semi-leptonic decay channel in the ATLAS experiment.

C. Benchouk, L. Hinz, E. Monnier
CPPM, CNRS/IN2P3 - Univ. Méditerranée, Marseille - France

Abstract

The study of spin correlation in $t\bar{t}$ events produced at the LHC can probe possible new physics in the strong production vertex. Effects of a few percent in the decay products observables and a high $t\bar{t}$ event production rate, expected during the first years of running of the ATLAS experiment, should allow the measurement of this correlation. This note presents the sensitivity of the ATLAS experiment to measure $t\bar{t}$ spin correlation in the channel $t\bar{t} \to WbWb \to \ell\nu bjjb$ and compares it to the dileptonic mode $t\bar{t} \to WbWb \to \ell\nu b\ell\nu b$.

1 Introduction

The top quark was first observed at Tevatron in 1994 by the CDF [1] and D0 [2] experiments. Its mass was measured to be 176±8±10 GeV and 199^{+19}_{-21}±22 GeV respectively. More precise measurements [3] lead to a mass of 174.3±5.1 GeV, a width $\Gamma(t \to W^+ b)$ of 1.5 GeV and a lifetime of $\tau_t \sim 5 \times 10^{-25}$ s. This lifetime is smaller than the hadronization time by an order of magnitude. Therefore, top quark decays before the hadronization can take place [4] and before the strong interaction has time to depolarise its spin [5, 6]. Thus spin properties of top quark can be studied in the decay products, as $t\bar{t}$ spin correlation.

With a rate per experiment of 8×10^6 $t\bar{t}$ events per year at low luminosity (10 fb^{-1}), the first three years at the LHC will allow the ATLAS and CMS experiments high statistic top physic studies. More precise top quark mass measurements as well as better sensitivity to spin correlation effects in angular distribution of top quark daughter particles can therefore be achieved. Such sensitivity to spin correlation effect can help us to probe new physics in the strong production vertex, for example CP violation in the Higgs sector [7]. A violation of the V–A structure of the charge current in tbW vertex can affect top quark decay particles observables.

This note is organized as follows : the production of polarized $t\bar{t}$, the top quark decay and the $t\bar{t}$ spin correlation are presented respectively in section 2, 3 and 4. Then section 5 and 6 deal with spin correlation effects in angular distributions of top quark daughter particles. Section 5 briefly remind existing dileptonic channel results [8]. Section 6 presents a complete study of the semileptonic channel. Finally, section 8 is devoted to general conclusions.

2 Polarized $t\bar{t}$ production

The two main $t\bar{t}$ production modes in hadronic colliders are the gluon-gluon fusion and $q\bar{q}$ annihilation. With a $t\bar{t}$ cross-section of 833pb [9], the pp LHC collider will produce, at low luminosity, more than 8 millions of $t\bar{t}$ events per year, mainly by the gluons fusion mode (90%). In comparison, the $p\bar{p}$ Tevatron collider will produce, for one year at 2 (30) fb^{-1} with $\sqrt{s} = 2$ TeV, 16000 (240000) $t\bar{t}$ events mainly by the $q\bar{q}$ mode (80%) [10].

In the helicity basis, for like-helicity (LL,RR)[1] or unlike-helicity (LR,RL) event, the $t\bar{t}$ polarization can be expressed for gluon-gluon fusion mode as [11] :

$$\frac{d^2\sigma_{LL,RR}(gg \to t\bar{t})}{d\beta d\cos\theta^\star} \sim \frac{7 + 9\beta^2\cos^2\theta^\star}{(1-\beta^2\cos^2\theta^\star)^2}(1-\beta^2)(1+\beta^2+\beta^2\sin^4\theta^\star) \quad (1)$$

$$\frac{d^2\sigma_{LR,RL}(gg \to t\bar{t})}{d\beta d\cos\theta^\star} \sim \frac{7 + 9\beta^2\cos^2\theta^\star}{(1-\beta^2\cos^2\theta^\star)^2}\beta^2\sin^2\theta^\star(1+cos^2\theta^\star) \quad (2)$$

and for $q\bar{q}$ annihilation as :

$$\frac{d^2\sigma_{LL,RR}(q\bar{q} \to t\bar{t})}{d\beta d\cos\theta^\star} \sim (1-\beta^2)\sin^2\theta^\star \quad (3)$$

$$\frac{d^2\sigma_{LR,RL}(q\bar{q} \to t\bar{t})}{d\beta d\cos\theta^\star} \sim 1+\cos^2\theta^\star \quad (4)$$

[1] L and R means respectively a left handed and a right handed t or $\bar{t}$ quark.

where $\theta^{\star}$ is the helicity angle in the $t\bar{t}$ rest frame and β the velocity (in c unit) of the top quark.

Equations 1 to 4 show that like and unlike helicity $t\bar{t}$ pair production are respectively suppressed for $\beta \to 1$ and for $\beta \to 0$. Thus, $t\bar{t}$ pairs are mainly produced with like helicities near threshold and unlike helicities for relativistic heavy quarks which leads to an helicity asymmetry (A) depending on the energy to produce $t\bar{t}$ pairs. This asymmetry is defined as :

$$A = \frac{N_{LL,RR} - N_{LR,RL}}{N_{LL,RR} + N_{LR,RL}} \tag{5}$$

where $N_{LL,RR}$ ($N_{LR,RL}$) is the number of like-helicity (unlike-helicity) pairs. At the LHC, with a pp center of mass energy of 14 TeV, the Standard Model predicts an asymmetry equal to 0.33±0.01 [8].

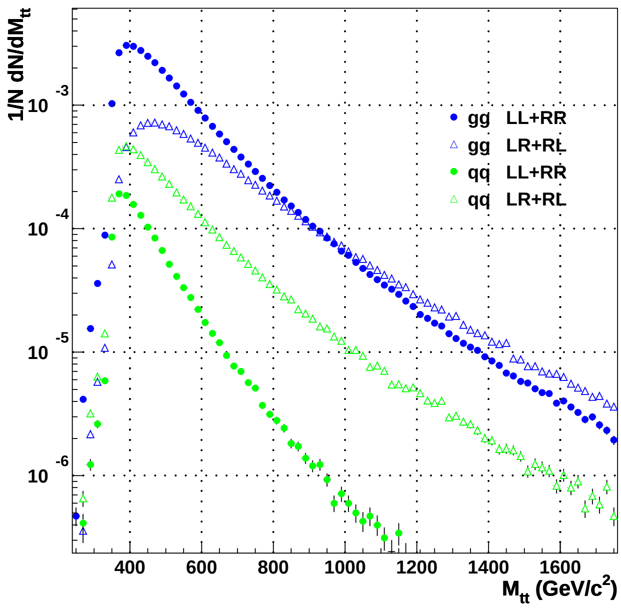

Figure 1: *The $t\bar{t}$ cross section as a function of the $t\bar{t}$ invariant mass (in GeV/c^2) for the four polarized $t\bar{t}$ production modes in the Standard Model case.*

The $t\bar{t}$ cross section versus the invariant $t\bar{t}$ mass ($M_{t\bar{t}}$) showed in Figure 1 for the two production modes and for the two $t\bar{t}$ helicities illustrates this suppression effects. This asymmetry, showed in Figure 2, is an important parameters in the observation of $t\bar{t}$ spin correlation from their decay products.

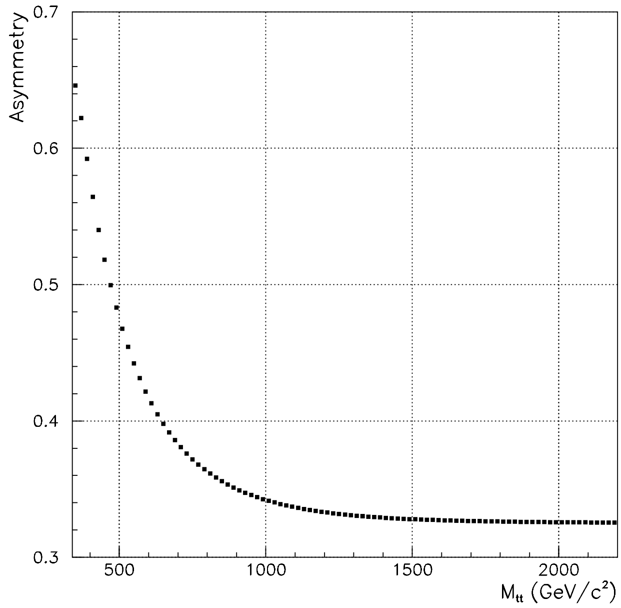

Figure 2: *Asymmetry of $t\bar{t}$ helicity for a set of events with an invariant $t\bar{t}$ mass little than $M_{t\bar{t}}$.*

3 Top decay

In the Standard Model, the top quark decays into a b quark and a real W boson with a branching ratio greater than 99%. The decay width is, at first order :

$$\Gamma(t \to bW^+) = \frac{G_F m_t^3}{8\pi\sqrt{2}} |V_{tb}|^2 \left(1 - \frac{M_W^2}{m_t^2}\right)^2 \left(1 + \frac{2M_W^2}{m_t^2}\right) \tag{6}$$

where M_W is the W mass, m_t the top mass, G_F the Fermi coupling constant and V_{tb} the Cabibbo-Kobayashi-Maskawa element matrix [12]. For a top mass of 174 GeV/c^2, $\Gamma(t \to bW^+)$ value is 1.5 GeV leading to a top lifetime of 0.5×10^{-24}s. As said in the introduction, this time is short compared to the hadronization time ($\sim$ 10 times greater) thus the top quark decays before hadronization [4, 6].

W bosons can decay into a lepton-neutrino pair or a quark-anti-quark pair. The final decay state for a top quark is then $t \to b\ell^+\nu_\ell$ or $t \to bq_1\bar{q}_2$ with respectively a branching ratio equal to 3/9 and 6/9.

In the Standard Model, the daughter particle directions are correlated with the top quark polarization which can be expressed in the top leptonic decay matrix element as :

$$|M|^2 \sim \frac{m_t^2 E_\ell (m_t - 2E_\ell)}{(q^2 - M_W^2)^2 + \Gamma_W^2 M_W^2} (1 - h \cos\theta_\ell^*) \tag{7}$$

where E_ℓ is the lepton energy, θ_ℓ^* the angle between lepton and top spin axis measured in the top rest frame, q is the sum of the 4-momenta of the lepton and of the neutrino and h

Particle	α	α for $m_t = 174$ GeV/c^2 and $M_W = 80.4$ GeV/c^2
$e^+, \bar{d}, \bar{s}$	1	1
ν, u, c	$\frac{(\xi-1)(\xi^2-11\xi-2)+12\xi\ln\xi}{(\xi+2)(\xi-1)^2}$	-0.326
W^+	$\frac{\xi-2}{\xi+2}$	0.4
b	$-\frac{\xi-2}{\xi+2}$	-0.4

Table 1: *Correlation coefficient, α, as a fonction of $\xi = m_t^2/M_W^2$ for right helicity top decay products with $m_b = 0$ approximation and for standard value of m_t and M_W [3, 19].*

is the correlation factor. In the Standard Model (SM) case $(h, \bar{h}) = (1, -1)$, whereas in a standard model without spin correlation (NC) these factors are $(h, \bar{h}) = (0, 0)$. These two models will be used in sections 5 and 6 to evaluate to efficiency of spin effect measurement.

The correlation between the top spin and the particle direction can be expressed in the angular distribution of decay products with respect to the top spin axis (defined as the top momentum direction in the top rest frame) [11] :

$$\frac{1}{N_{tot}}\frac{dN}{d\cos\theta_i^*} = \frac{1}{2}(1 + \alpha_i \cos\theta_i^*) = f_{\alpha_i}(\cos\theta_i^*) \tag{8}$$

where θ_i^* is the angle between the top spin axis and the particle i, and α_i is the correlation coefficient, given in Table 1 for the Standard Model case. Using the standard value of m_t and M_W [3, 19], for a top quark with a right helicity, α is equal to 1, i.e. h, for lepton ℓ^+, $\bar{d}$ or $\bar{s}$, -0.326 for neutrino, u or c quark, -0.4 and 0.4 respectively for b and W^+. The sign of α depends on top helicity and one obtain the following relation between correlation coefficients :

$$\begin{aligned} \alpha_i^R &= -\alpha_i^L \\ \bar{\alpha}_i^R &= -\bar{\alpha}_i^L \\ \bar{\alpha}_i^R &= \alpha_i^L \\ \bar{\alpha}_i^L &= \alpha_i^R \end{aligned}$$

where, for example, $\bar{\alpha}_i^L$ denotes the correlation coefficient of particle i coming from an anti-top with a left helicity. The angular distribution of equation 8 in the Standard Model case for daughter particles of a top with right helicity is represented in Figure 3. The shaded squares are in the case of a left helicity top.

Since the top quark is produced without prefered polarization, the number of top quark with right helicity, written t_R, and left helicity, t_L, is the same. This is integrated when calculating the probability (P_i^R) that a top daughter particle i (for example a lepton ℓ^+), comes from a t_R :

$$P_i^R = \frac{\int_{-1}^{1} f_{\alpha_i^R}(\cos\theta_i^*)\ \mathrm{d}\cos\theta_i^*}{\int_{-1}^{1} f_{\alpha_i^R}(\cos\theta_i^*)\ \mathrm{d}\cos\theta_i^* + \int_{-1}^{1} f_{\alpha_i^L}(\cos\theta_i^*)\ \mathrm{d}\cos\theta_i^*} = \frac{1}{2} \tag{9}$$

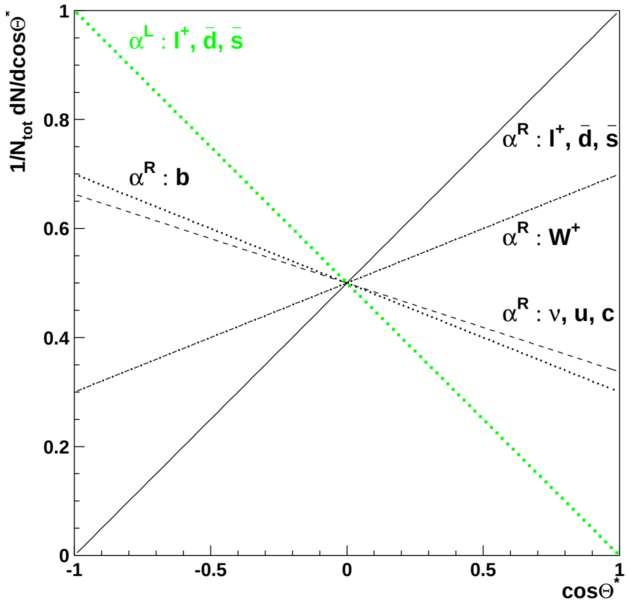

Figure 3: *Angular distributions of top decay products with right helicity (full, dashed and dotted lines) and with left helicity (shadded square) in the Standard Model case. These distributions depend on each particle α value.*

Thus P_i^R is equal to P_i^L. Placing in the experimental conditions, i.e. the two top polarizations are undistinguishable, the decay product angular distribution is $P_i^R \times (1 + \alpha_i^R \cos\theta_i^*)/2 + P_i^L \times (1 + \alpha_i^L \cos\theta_i^*)/2 = 1/2$. We can conclude that the correlation between the top helicity and the decay product direction cannot be viewed through the daughter particle angular distributions in the experimental conditions. But the probability to have a lepton ℓ^+ coming from a t_R, in a set of events with one ℓ^+, increases if $\cos\theta_{\ell^+}^* > y$, y is a given value in $]-1,1[$. Then, replacing the -1 limit by y in equation 9 leads to:

$$P_{\ell^+}^R(y) = \frac{2 + \alpha_{\ell^+}^R(1+y)}{4} \tag{10}$$

where $P_{\ell^+}^R(y)$ is the probability to have a lepton ℓ^+ coming from a t_R if $\cos\theta_{\ell^+}^* > y$. In other words, this is the proportion of t_R ($P_{t_R} = P_{\ell^+}^R(y)$) in the set of selected events (with one ℓ^+ and for $\cos\theta_{\ell^+}^* > y$). For example, if $y = 0$, then $P_{\ell^+}^R(0) = 3/4$, meaning that 75% of top have right helicity and 25% left helicity. Since the $t\bar{t}$ pairs are by a majority produced with the same helicity (leading to the asymetry $A = 0.33$) the number of right helicity anti-top ($\bar{t}_R$) is greater than the number of left helicity anti-top ($\bar{t}_L$). A general equation which give the proportion of $\bar{t}_R$ and $\bar{t}_L$ when the proportion of t_R is P_{t_R} can be derived from eq. 5 as

$$P_{\bar{t}_R} = \frac{1 - A(1 - 2P_{t_R})}{2} \tag{11}$$

$$P_{\bar{t}_L} = \frac{1 + A(1 - 2P_{t_R})}{2} \tag{12}$$

This implies an angular distribution of $\bar{t}$ daughter particle, j, as :

$$\frac{1}{N_{tot}} \frac{dN}{d\cos\bar{\theta}_j^*} = \frac{1 + \bar{\alpha}_j^L A(1 - 2P_{t_R})\cos\bar{\theta}_j^*}{2} \tag{13}$$

To reveal a correlation between top helicity and top decay product direction and measure α value, a selection of events in one side of $t\bar{t}$ is necessary to extract the slope of the angular distribution of particle in the other side. The effect is diluted due to the asymmetry A and can be increased by selecting events, for example using a cut on the invariant $t\bar{t}$ mass $M_{t\bar{t}}$. In other words, there is a correlation between t daughter particle and $\bar{t}$ daughter particle direction due to : *i*) a correlation between top spin helicity and decay particle direction and, *ii*) a $t\bar{t}$ spin correlation leading to an asymmetry A defined in section 2.

4 Spin correlation in $t\bar{t}$ events

Combining the $t\bar{t}$ spin correlation in production, section 2, and the conservation of spin information in decay products, section 3, an angular correlation between decay products coming from the top and anti-top quark is expected and given by [11] :

$$\frac{1}{N_{tot}} \frac{d^2N}{d\cos\theta_i^* \, d\cos\bar{\theta}_j^*} = \frac{1}{4}(1 + \kappa\cos\theta_i^*\cos\bar{\theta}_j^*) \tag{14}$$

where θ_i^* ($\bar{\theta}_j^*$) is the angle of the t ($\bar{t}$) decay product i (j) with respect to the top (anti-top) spin axis in the top (anti-top) rest frame and κ is

$$\kappa = A\alpha_i\bar{\alpha}_j \tag{15}$$

In the case of spherical decay of t and $\bar{t}$ quark, i.e. no correlation between top spin and daughter particle direction, $\kappa = 0$ and Eq. 14 is 1/4. The effect of spin correlation on angular distribution depends on both the asymmetry A and particle type. The higher effect will be viewed for leptonic decay $t\bar{t} \to W^+bW^-\bar{b} \to \ell^+\nu_\ell b\ell^-\bar{\nu}_\ell\bar{b}$ and for a pure like-helicity $A = 1$. At the LHC, the total asymmetry A is 0.33 (sect. 2), corresponding to a κ of $0.33 \times 1 \times (-1) = -0.33$ in dileptonic channel. Nevertheless, it is possible to increase the like-helicity purity selecting $t\bar{t}$ events in a invariant mass $M_{t\bar{t}}$ range as Figure 1 suggests it. Figure 2 shows the asymmetry A as a function of invariant mass below $M_{t\bar{t}}$. For example, asymmetry is 0.42 if $t\bar{t}$ events have a $t\bar{t}$ invariant mass below 600 GeV/c^2.

Figures 4**a**-**c** show the angular distribution described in Eq. 14 for the semileptonic events $t\bar{t} \to WbWb \to \ell\nu_\ell bjjb$ for three combination of particles : **a**- between lepton ($e^\pm$ or $\mu^\pm$) and down quark, **b**- between lepton and u quark and **c**- between lepton and d and u quark. In this three cases, κ is respectively -0.33, 0.108 and -0.111 for $A = 0.33$. These different values come from the correlation coefficient α function of the particle type. In experimental conditions, light quarks flavor are not easily distinguishable, so case 4c and the corresponding κ are the reference for the semileptonic chanel.

Before presenting the study of spin correlation in a given channel, some considerations are needed, on statistics and background. The dileptonic channel has the highest correlation ($\kappa = -0.33$) and the lowest background [15]. But, as shown in Table 2, this channel suffer from the lowest statistic. The semileptonic channel has a smaller correlation value than the dileptonic channel ($\kappa = -0.111$) but has a higher statistic. The background is more important but can be efficiently reduced [15]. The hadronic channel has the lowest correlation coefficient ($\kappa = -0.04$) and the largest background [15]. Although the statistic is the highest, this channel seems far less promising for spin correlation studies, leaving only the first two cases to study.

5 Spin correlation effect in angular distribution of decay products in the dileptonic channel : $t\bar{t} \to W^+bW^-\bar{b} \to \ell^+\nu b\ell^-\bar{\nu}\bar{b}$

Dileptonic samples were studied by V. Simak, J. Smolik and A. Lagatta [8]. Their results show the possibility to measure spin correlation effects through the angular distribution, in the laboratory frame, between the lepton (e^+, μ^+) coming from a top and the lepton (e^-, μ^-) coming from the anti-top. In order to be able to compare this channel to the semileptonic channel, we have repeated their study with events generated with the same modified version of PYTHIA 5.7 [16] that incorporates spin correlation. Default Pythia parameters are used but initial and final state radiations (ISR, FSR) are off as in [8]. Events were reconstructed with a fast detector simulation : ATLFAST 2.22 [17].

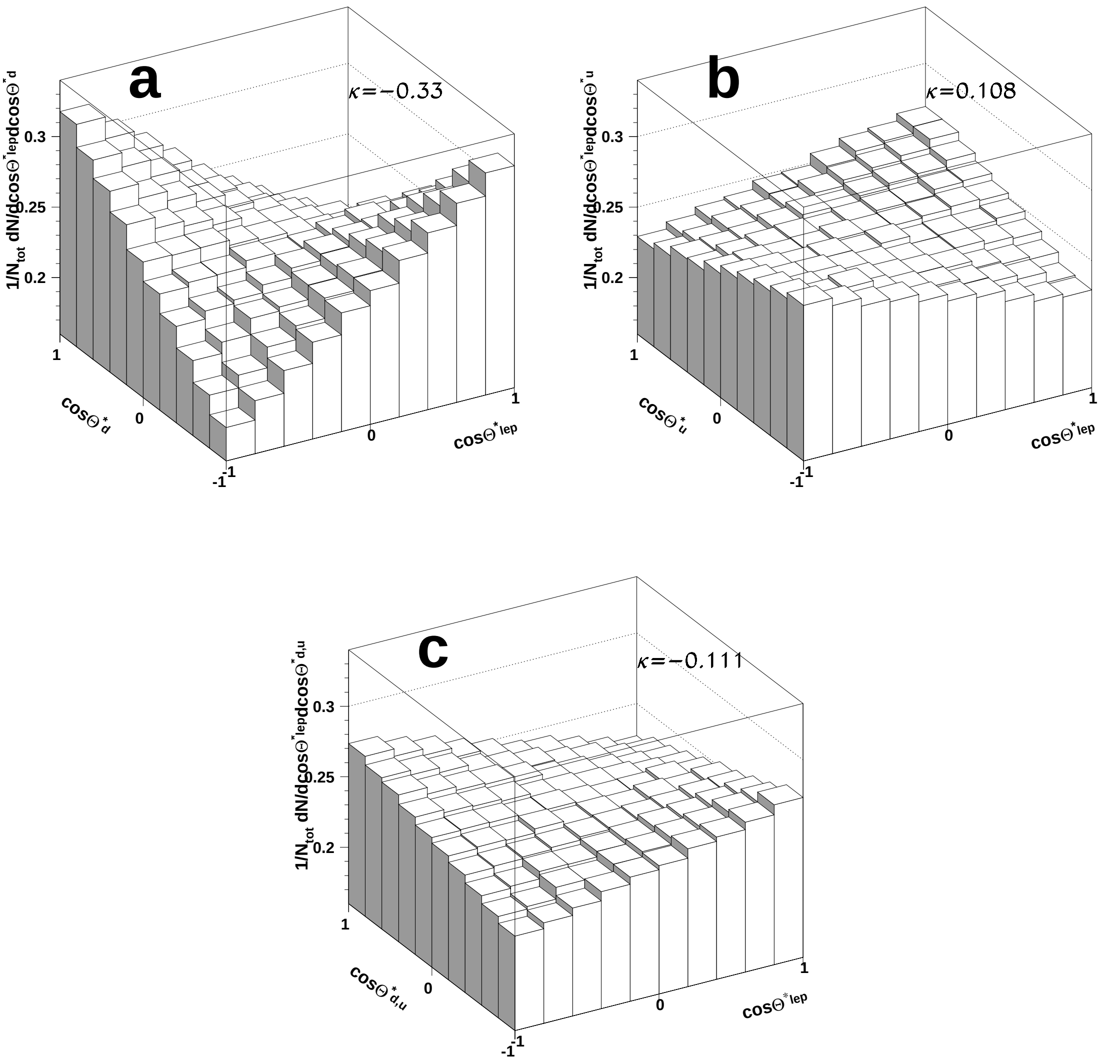

Figure 4: *Angular distribution of outgoing particles from t and $\bar{t}$ predicted by the Standard Model :* **a***- angle between lepton ($e^{\pm}$, $\mu^{\pm}$) and down quark,* **b***- angle between lepton and up quark,* **c***- angle between lepton and down or up quark.*

Channel	Branching ratio	Events for 1 year low lumonisity (10 fb^{-1})
Dileptonic $\ell^+\nu_\ell\bar{b}\ell^-\bar{\nu_\ell}b$ $(\ell = e, \mu)$	4/81	$\sim 0.4 \times 10^6$
Semileptonic $\ell\nu_\ell bq\bar{q}b$ $(\ell = e, \mu)$	24/81	$\sim 2.4 \times 10^6$
Hadronic $q\bar{q}bq\bar{q}\bar{b}$	36/81	$\sim 3.6 \times 10^6$

Table 2: *Branching ratio for the different decay channel. τ channel is not treated in spin correlation studies.*

Because of two neutrinos in final decay products which implies a difficult top frame reconstruction, the spin correlation effect is measured in variables in the laboratory frame $\cos\theta_{\ell\ell}$ and $\phi_{\ell\ell}$, the polar and azimuthal angle between the two lepton. For one year at low luminosity and applying the following cuts (same as in Ref [8] p.6-7) :

- two high p^T isolated and opposite-sign lepton with $|\eta| < 2.5$
- $p^T_\ell > 35, 25$ GeV/c
- in case of $e^+e^-, \mu^+\mu^-$: $|m_{\ell\ell} - m_Z| > 10$ GeV/c^2
- $p^T_{miss} > 40$ GeV/c
- two jets with $p^T_j > 15$ GeV/c

we obtain, in Figure 5, the same results. The Figure 5**a-b** shows distributions of $\cos\theta_{\ell\ell}$ and $\phi_{\ell\ell}$ for the Standard Model correlation (SM) and for a model without correlation (NC) and Figure 5**c-d** the fractionnal difference between the two models. The maximum spin correlation effect between SM and NC is about 5% and 3% for $\phi_{\ell\ell}$ and $\cos\theta_{\ell\ell}$ respectively. Only statistical errors are given. These results are reminded in order to be compared to the semileptonic channel.

In order to compare the two channels (semileptonic and dileptonic), a spin correlation identification power estimator, χ^2/ndf, is defined from the fractionnal difference between the two models (SM and NC), as :

$$\chi^2/ndf = \frac{1}{N_{bin}} \sum_{i=1}^{N_{bin}} \frac{\left(\frac{F_i^{SM}(x) - F_i^{NC}(x)}{F_i^{SM}(x)}\right)^2}{\sigma_i^2(x)} \ , \quad x = \cos\theta, \phi \tag{16}$$

where F_i^Y is the value of the angular distribution ($1/N_{tot}\ dN/dx$) of the model Y for the bin i, $\sigma_i(x)$ is the error of the fractional difference computed for the bin i and N_{bin}

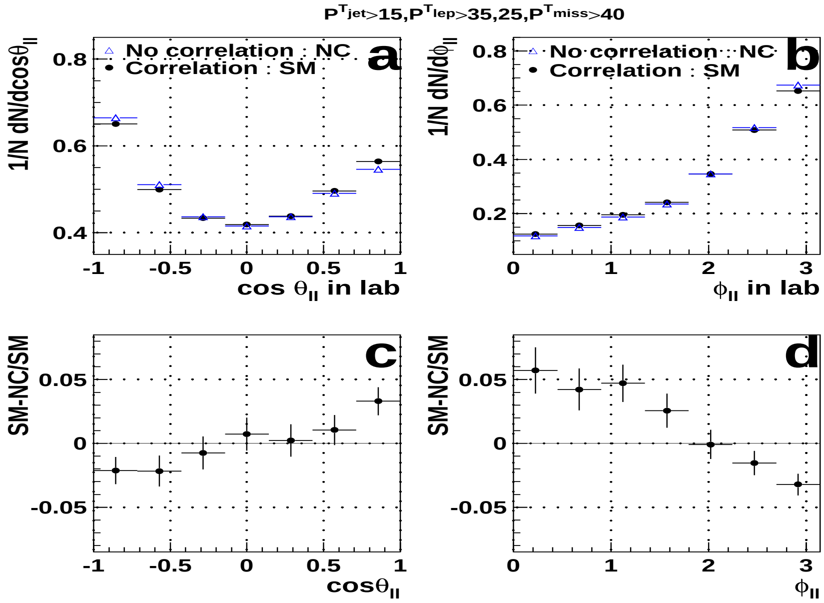

Figure 5: *Angular distributions of* $\cos\theta$ *(a) and* ϕ *(b) between the 2 leptons for Standard Model and a model without spin correlation. c) and d) shows the fractionnal difference between the distributions of the two models.*

	χ^2/ndf	
	$\cos\theta_{\ell\ell}$	$\phi_{\ell\ell}$
$\kappa_{SM} = -0.33$, $\kappa_{NC} = 0$	2.5	6.8

Table 3: *Value of estimator* χ^2 *to distinguish two models, here the Standard Model and a model without correlation, for the dileptonic channel.*

the number of bins. A χ^2/ndf smaller or equal to the unity implies that the two models are not distinguishable. Table 3 gives the value of χ^2/ndf which compares the SM (with $\kappa = -0.33$) to NC ($\kappa = 0$). As already seen in Figure 5, the most significative variable is $\phi_{\ell\ell}$ because of it is less sensitive to the boost of the top rest frame than $\theta_{\ell\ell}$. It results in the χ^2/ndf value more than twice higher for ϕ as for the other variable.

These results do not take into account ISR and FSR. Radiation may influence the angular distributions and dilute the spin correlation effect. Nevertheless, assuming that this dilution is negligeable in the dileptonic channel, which has to be confirmed, these results will serve as reference in the comparison with the semileptonic channel.

6 Spin correlation effects in angular distribution of decay products in the semileptonic channel : $t\bar{t} \to W^+bW\bar{b} \to \ell\nu bjjb$

Compared to the dileptonic channel, this channel has a big statistical advantage, as seen in Table 2. The number of events produced is 6 times higher than for dileptonic channel. But the κ value is smaller, because of misidentification of light quarks, and equal to -0.111 $(0.33 \times (1 \times (-1) + 1 \times 0.326)/2)$ if the proportion of up and down type quark is equal. Moreover, initial (ISR) and final state radiation (FSR) as well as background are expected to play a bigger role than for the dileptonic channel and are going to dilute the effect of spin correlation in angular distributions.

After having defined selection criteria, a set of events without radiation and without background (section 6.2) is studied. All these competing effects impacts on the sensitivity of detection of the spin correlation effects with this channel. Then, in section 6.3, ISR, FSR and background are added.

To compare results with dileptonic channel, the equivalent of one year at low luminosity of $t\bar{t}$ pairs were produced, i.e. 8 millions of events (all channels) for the two models in the two cases : with or without radiation.

6.1 Selection of events

Events are selected with at least 4 jets (reconstructed in a ΔR cone of 0.7). Two of these jets are tagged as b-jets with an efficiency of 60% per b and a rejection factor of 100. In addition, one isolated lepton is required. A fiducial cut is applied on the pseudo-rapidity of the lepton and the jets : $|\eta| < 2.5$. Typical transverse momentum constraints are then applied as in [18] :

- Lepton : $p_\ell^T > 20$ GeV/c
- Jet : $p_j^T > 20$ GeV/c
- Missing energy : $p_{miss}^T > 20$ GeV/c

For events with a number of non b jets greater than 2 jets, the selected pair is the one with the closest invariant mass to the W mass ($M_W = 80.4$ GeV/c^2 [19]).

Among all selected jets, if the number of non b jets are greater than 2, then the pair of jets is the one which have an invariant mass closest to the W mean mass ($M_W = 80.4$ GeV/c^2). In addition, only events with a jet pair invariant mass within 20 GeV/c^2 of the known W mass are kept to reduce background and to avoid bad reconstructed events.

6.2 Spin correlation effect without radiation and background

The distribution of the cosine of the polar angle ($\cos\theta_{\ell j}$) in the laboratory frame between the lepton coming from one of the top quark and one jet coming from the other top quark for the two model (SM and NC) is shown in Figure 6a. The azimuthal angular distribution $\phi_{\ell j}$ for these two particles and for the two models is shown in 6b. Since there

	χ^2/ndf	
	$\cos\theta_{\ell j}$	$\phi_{\ell j}$
No ISR, No FSR, No BCK ($\kappa_{SM} = -0.111$, $\kappa_{NC} = 0$)	3.3	5.7

Table 4: *Spin correlation identification power estimator, χ^2/ndf between the two models, here the Standard Model with and without correlation, for the semileptonic channel.*

is no light quarks identification, the two selected jets are mixed in the distribution. We have the same number of jets with $|\alpha| = 1$ and $|\alpha| = 0.326$.

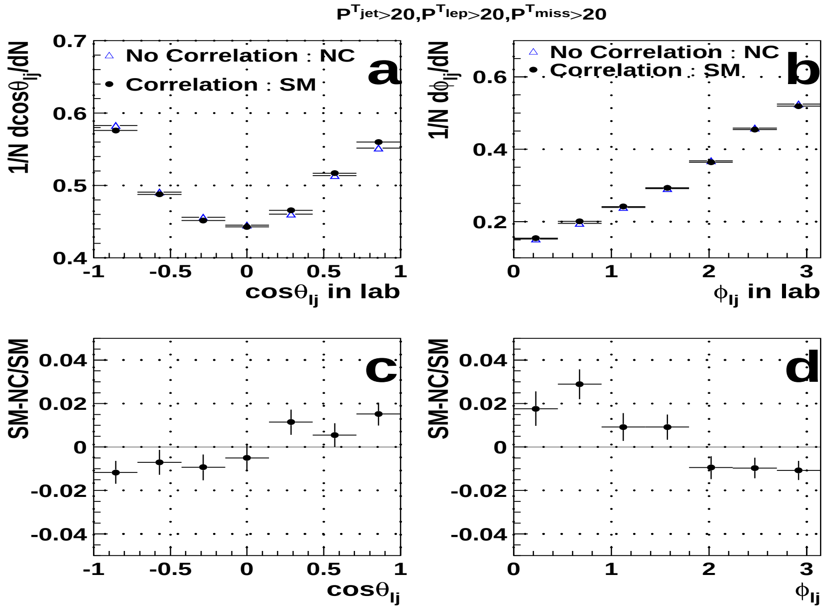

Figure 6: *Angular distributions of* $\cos\theta$ *(a) and* ϕ *(b) between lepton and jet for Standard Model with and without spin correlation. c) and d) shows the fractional difference between the distributions of the two models.*

Figures 6**c-d** show the fractional difference of angular distributions between the two models. A maximum effect of 2-3% is observed for ϕ and about 1.5% for $\cos\theta$. The spin correlation effect follows a similar shape as dileptonic channel with lower amplitude but with lower errors. Error bars are only statistical errors. Values of the spin correlation identification power, defined in section 5 as χ^2/ndf, are given in Table 4. They are about the same as for the dileptonic channel at this step of analysis, without initial (ISR) and final (FSR) radiation and without background (BCK).

These results are compared with theory in Figure 7 that shows the two angular distribution in the laboratory frame for one year at low luminosity without detector acceptance. A maximum effect of 1.5% is expected. The comparison of Figure 7 and 6 show

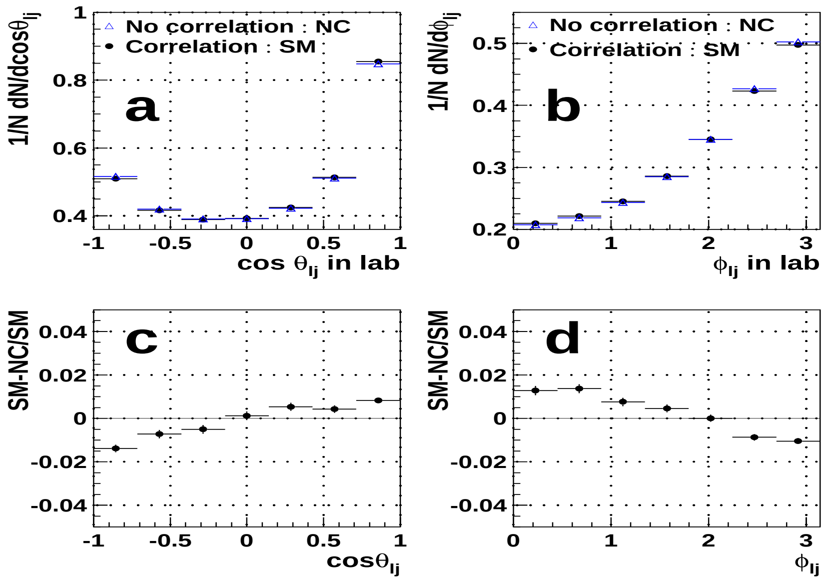

Figure 7: *Angular distributions of* $\cos\theta_{\ell j}$ *(a) and* $\phi_{\ell j}$ *(b) in the laboratory frame expected from the theory (Pythia, no radiation, no hadronization) of the two models for one year at low luminosity. c) and d) are the fractionnal difference between SM and NC models.*

that **a**-**b** distributions are distorted, due to acceptance effects, and that **c**-**d** distributions have a similar shape with compatible amplitude.

6.3 Spin correlation effect in angular distribution including radiation and background

6.3.1 Background study

Principal sources of background are channels $W + f$, $W + g$, $b\bar{b}$, $\gamma^*/Z^0 + f$, $\gamma^*/Z^0 + g$ and γ^*/Z^0. Smaller cross-section sources of background are also included in the analysis : $Wb\bar{b}$, Z^0Z^0, Z^0W and WW. Begining with a background rate six times higher than signal at production level, backgrounds can be easily reduced, to the signal level, when at least 4 jets ($|\eta| < 2.5$) with 2 b-tagged jets and one isolated lepton ($|\eta| < 2.5$) are required. Adding cut on the jet pair invariant mass, $|M_{jj} - M_W| < 20$ GeV/c^2, background is reduced by a factor 2.

Since $t\bar{t}$ events have high transverse momentum in comparison to the background, cuts on transverse momentum are applied to increase the background rejection. Such cuts are studied. Begining the p^T cuts applied on lepton, neutrino and jets transverse momentum from their identification of isolated particle/jet values, Figures 8**a**-**b** show the number of $t\bar{t}$ and background events as a function of various p^T cuts applied :

- 4 cuts on p_j^T : 15, 20, 30, 40 GeV/c. A constant cut on p_j^T is applied on each region

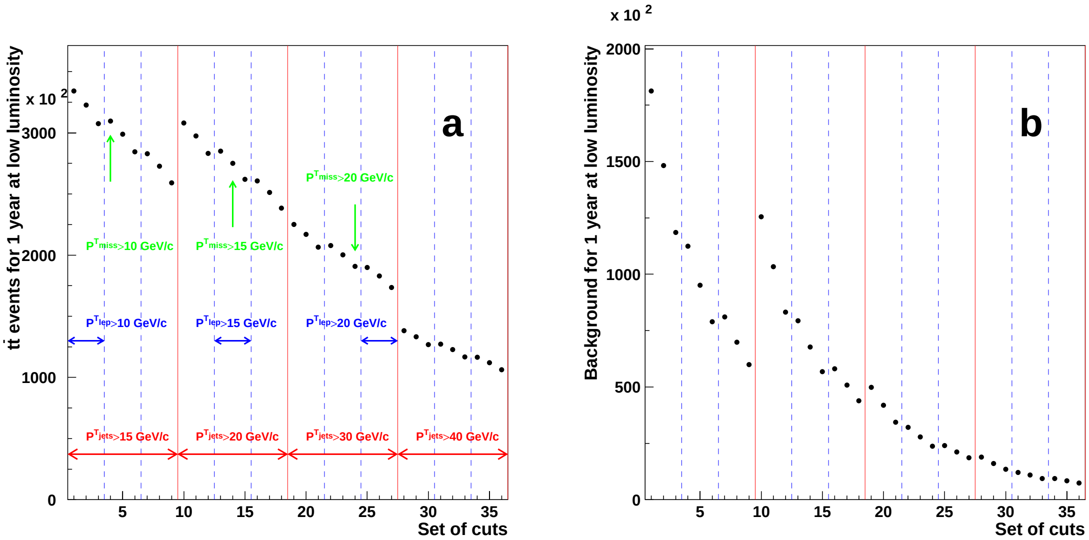

Figure 8: *Number of $t\bar{t}$ events (a) and background (b) as a function of sets of cuts for one year at low luminosity. Vertical full and dashed lines define zones with constant p^T cuts.*

in Figure 8 defined by the vertical full lines.

- 3 cuts on p_ℓ^T : 10, 15, 20 GeV/c. A constant cut on p_ℓ^T is applied on each region in Figure 8 defined by the vertical dashed lines.
- 3 cuts on p_{miss}^T : 10, 15, 20 GeV/c. The cut varies in each zone delimited by the dashed lines in Figure 8.

In order to measure the predicted small spin correlation effects, high statistics are needed. Thus, a compromise between high $t\bar{t}$ statistics and low background has to be found. Figures 9 show the ratio S/$\sqrt{B}$ which give an idea of the compromise. The cut $(p_j^T, p_\ell^T, p_{miss}^T) > (30, 20, 20)$ GeV/c give the best S/$\sqrt{B}$. This set of cut is therefore choosen for the analysis. But, another interesting set of cuts is $(p_j^T, p_\ell^T, p_{miss}^T) > (20, 20, 20)$ GeV/c. It allows to increase the number of $t\bar{t}$ by 30% compared to $(p_j^T, p_\ell^T, p_{miss}^T) > (30, 20, 20)$ GeV/c, corresponding to more than 200 000 $t\bar{t}$ per year at low luminosity (Fig. 8**a**).

Thus, two sets of cut are choosen to measure the spin correlation effect in decay products angular distribution : $(p_j^T, p_\ell^T, p_{miss}^T) > (20, 20, 20)$ GeV/c (Set 1) and $(p_j^T, p_\ell^T, p_{miss}^T) > (30, 20, 20)$ GeV/c (Set 2). Table 5 gives the number of background events and the S/$\sqrt{B}$ for these two sets and Figures 10**a-d** show the corresponding distribution of $\cos\theta_{\ell j}$ and $\phi_{\ell j}$ in laboratory for signal and background. Background distributions are relatively flat for $\phi_{\ell j}$ compared to signal variation. The cosine distribution is almost flat between [-0.8,0.8]. Thus the background impact is expected to be greater on the $\cos\theta_{\ell j}$ distribution than for $\phi_{\ell j}$, especially for $|\cos\theta_{\ell j}| > 0.8$.

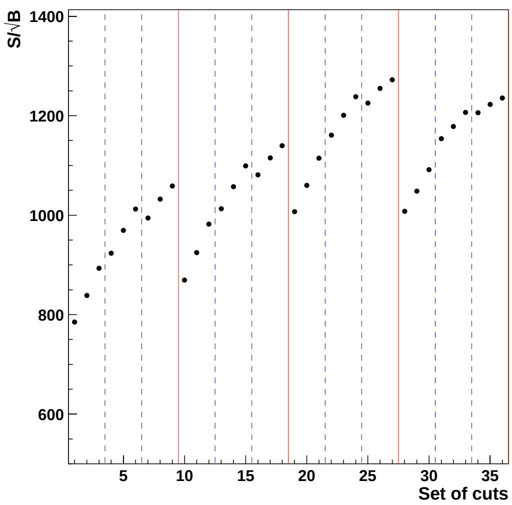

Figure 9: *Signal over the root mean square of background $S/\sqrt{B}$ for the various set of cuts.*

Channel	Cross section (pb)	Events per 10 fb^{-1} more than 4 jets whose 2 b + 1 lepton $+\lvert M_{jj}-M_W\rvert$<20 GeV/c^2 + $\lvert\eta\rvert < 2.5$	Set 1 (20,20,20)	Set 2 (30,20,20)
$b\bar{b}$	1.93×10^8	94896	6792	2848
γ^*/Z^0	1×10^6	2984	496	160
$W+g$	1.71×10^5	2288	872	288
$W+f$	1.31×10^5	57400	31240	13496
γ^*/Z^0+g	6.86×10^4	2376	520	272
γ^*/Z^0+f	6.18×10^4	21016	3736	1496
WW	70.3	148	88	46
$Wb\bar{b}$	66.7	75	34	10
Z^0W	26.3	101	51	27
Z^0Z^0	10.5	40	9	6
Total	1.94×10^8	181324	43838	18649
S/$\sqrt{B}$ after cuts		784	1139	1271

Table 5: *Cross section and number of background events per one year at low luminosity for different sets of cuts and the corresponding $S/\sqrt{B}$ ratio.*

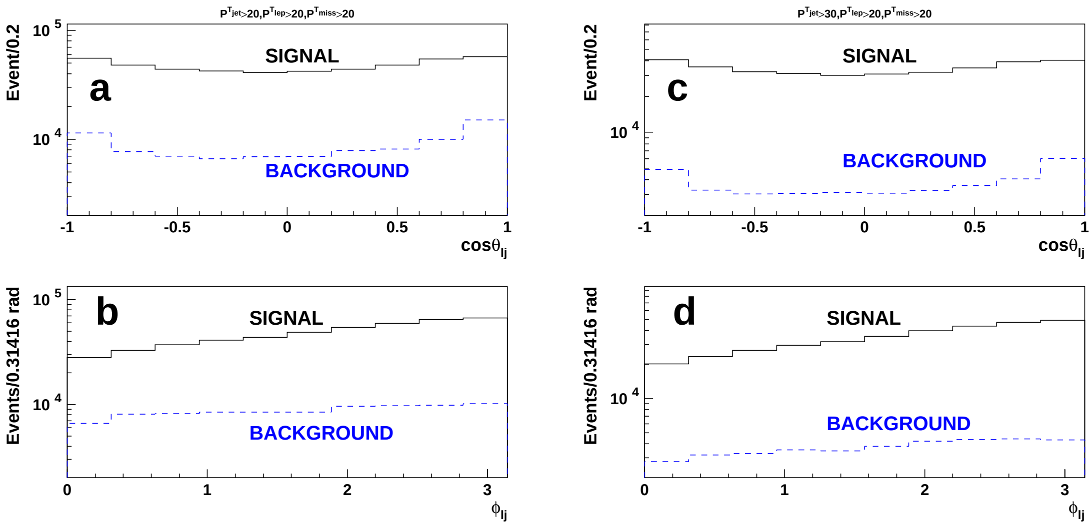

Figure 10: *Angular distribution of signal (full line) and background (dashed line) for the two choosen sets of cuts, in vertical logarithmic scale.* **a**-**b** $(p_j^T, p_\ell^T, p_{miss}^T) > (20, 20, 20)$ *GeV/c and* **c**-**d** $(p_j^T, p_\ell^T, p_{miss}^T) > (30, 20, 20)$ *GeV/c.*

6.3.2 Angular distribution in laboratory frame

Initial and final state radiations induce energy leakage and a mismeasurement of the jet directions. The angle determination between particles is not as precise as without radiation. Thus, a decrease of the spin effect is expected in angular distributions. With the background added, a few percent effect can be less visible, or not visible compared to the cleaner dileptonic channel.

Figures 11 (12) show the angular distributions for SM and NC models and the corresponding fractional difference when initial and final state radiation are included and using the set 1 (2) of cuts. Differences between the two models is smaller than for the "no radiation" case, the cosine is more affected by ISR and FSR than the azimuthal angle measurement. Nevertheless, we still can distinguish between the two models using the $\phi_{\ell j}$ angle after one year at low luminosity by at least 2σ.

Figures 13 (14) are obtained when backgrounds are included. Comparing Figure 13a and Figure 11a, it shows that backgrounds influence the cosine distribution in increasing the number of events for $|\cos\theta_{\ell j}| > 0.8$. The fractionnal difference between the models is slightly less pronounced than in the case without background.The larger effect, for ϕ, is 1.5% for the two sets of cut. The spin correlation identification power estimator χ^2/ndf decreases by a factor 1.2 (1.1) but keep a value greater than 2σ for the cut set 1 (2). Values of the correlation identification power estimator are summarized in Table 6 for the three cases of semileptonic channel (no radiation, radiations with or without background). The set 2, given angular distributions with higher statistical fluctuation than set 1, can be more efficient than set 1 after three year at low luminosity.

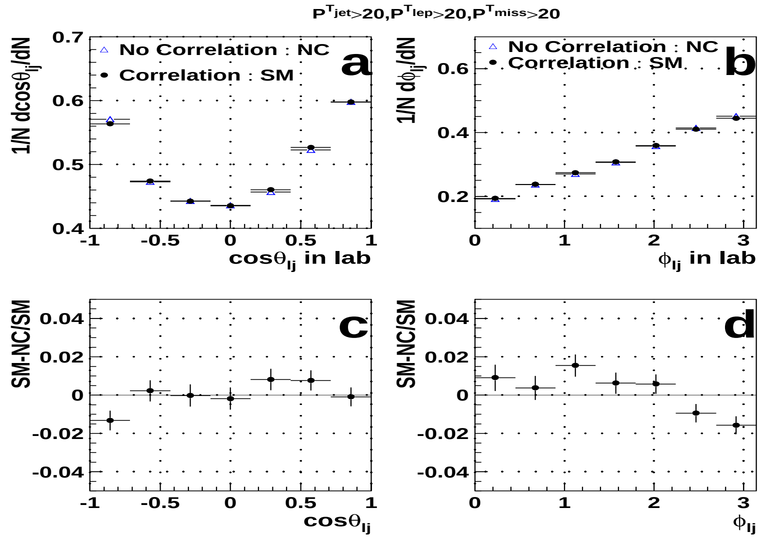

Figure 11: *Angular distributions of* $\cos\theta$ *(a) and* ϕ *(b) between lepton and jet for Standard Model and a model without spin correlation. c) and d) show the fractional difference between the distributions of the two models. ISR and FSR are included in analysis and the set 1 of cuts is used.*

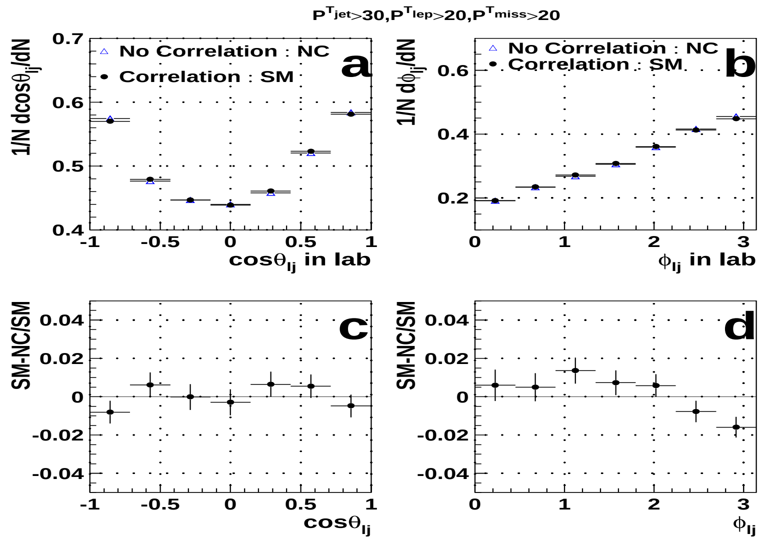

Figure 12: *Angular distributions of* $\cos\theta$ *(a) and* ϕ *(b) between lepton and jet for Standard Model and a model without spin correlation. c) and d) show the fractional difference between the distributions of the two models. ISR and FSR are included in analysis and the set 2 of cuts is used.*

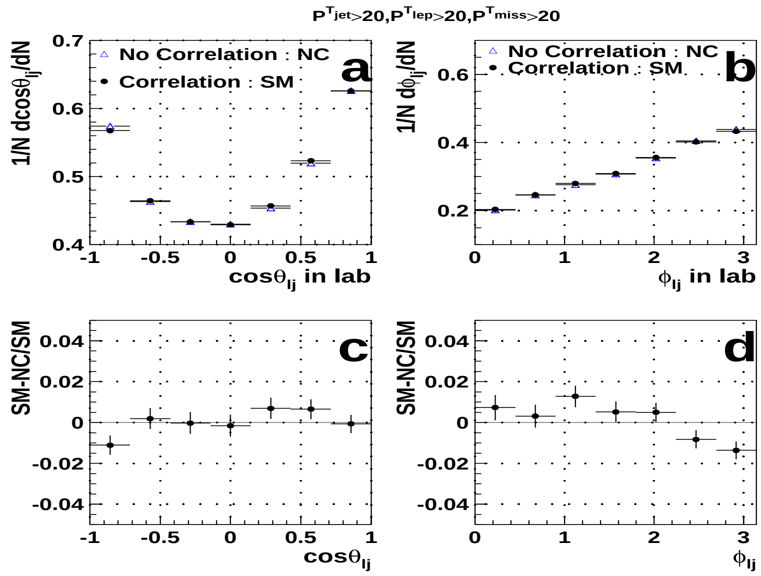

Figure 13: *Angular distributions of* $\cos\theta$ *(a) and* ϕ *(b) between lepton and jet for Standard Model and a model without spin correlation. c) and d) shows the fractional difference between the distributions of the two models. ISR,FSR and background are included in analysis and the set 1 of cuts is used .*

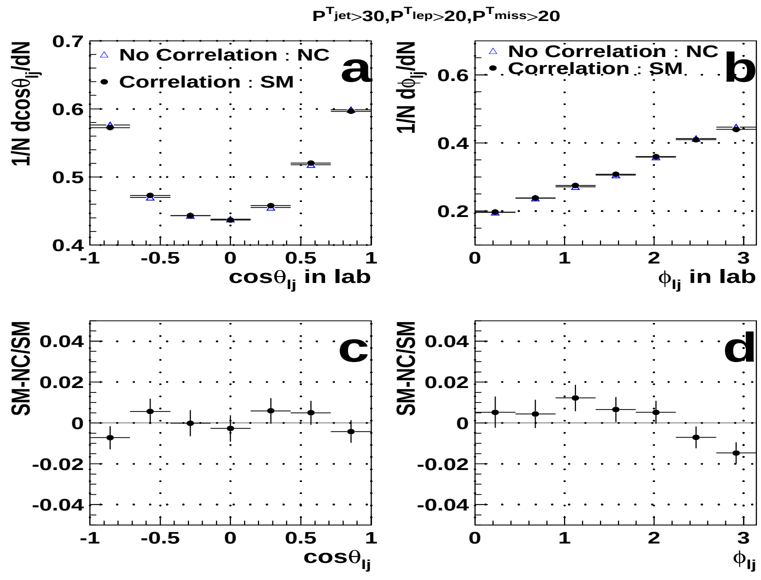

Figure 14: *Angular distributions of* $\cos\theta$ *(a) and* ϕ *(b) between lepton and jet for Standard Model and a model without spin correlation. c) and d) shows the fractional difference between the distributions of the two models. ISR,FSR and background are included in analysis and the set 2 of cuts is used .*

	χ^2/ndf	
	$\cos\theta_{\ell j}$	$\phi_{\ell j}$
ISR, FSR ($\kappa_{SM} = -0.111$, $\kappa_{NC} = 0$)		
Set 1 : $(p_j^T, p_\ell^T, p_{miss}^T) > (20, 20, 20)$ GeV/c	1.6	3.9
Set 2 : $(p_j^T, p_\ell^T, p_{miss}^T) > (30, 20, 20)$ GeV/c	0.8	2.5
ISR, FSR + BCK ($\kappa_{SM} = -0.111$, $\kappa_{NC} = 0$)		
Set 1 : $(p_j^T, p_\ell^T, p_{miss}^T) > (20, 20, 20)$ GeV/c	1.3	3.3
Set 2 : $(p_j^T, p_\ell^T, p_{miss}^T) > (30, 20, 20)$ GeV/c	0.7	2.3

Table 6: *Value of the correlation identification power estimator χ^2/ndf for the semileptonic channel with radiation, with or without background.*

As a conclusion, it is possible to distinguish the effect of spin correlation when the deviation is maximum (Standard Model compared with the Standard Model without spin correlation) after one year at low luminosity, using the angular distributions. The effect of spin correlation is higher for the azimythal angle ϕ since it is less affected by the boost of top rest frame and the radiations than the polar angle. Three years of run are certainly nedeed to have a significant effect in polar angle distribution.

In order to distinguish deviation with respect to the Standard Model due to signatures of new physics, with spin correlation not equal to 0, higher sensitivity is required. Sensitivy is described by the error values or by the the correlation identification power estimator. These errors vary from 0.7% to 0.5% for an expected maximum spin effect of 1.5% when cut set 1 is used in experiment condition (ISR+FSR+Background) leading to a χ^2/ndf equal to 3. After 3 years at low luminosity, statistical errors decrease to 0.4% in the first bin until 0.3% in the last bin. With these errors values, we are able to measure a deviation of the Standard Model of 0.8% with a statistical significance greater than 2σ.

These measurements can be enhance in explaining the angular distribution of particles in the top rest frame which is higher sentivitive to the correlation parameters A and α, i.e. κ.

6.3.3 Angular distribution in top rest frame

A direct measurement of κ can be performed. With only one neutrino in this channel, it is possible to reconstruct decay particles momenta in top and anti-top rest frame and thus to have similar angular distribution as in Figure 3 (taking into account top ambiguity, selection criteria and the ambiguity of the two jets which have different α value) and Figure 4c. Using set 1 cuts, one obtains, at the generation level (Pythia) without radiation and without background, the Figures 15 and 16.

Figure 15 shows the jet angular distribution in top or anti-top rest frame described by equation 13 when $\cos\theta^*$ of the lepton is greater than 0. SM and NC case distribution are presented as well as the corresponding fractionnal difference. Acceptance effects distort the expected straight line, whose slope is to -0.0556 (0.0) for SM (NC). More precisely, η fiducial cut has a minimal cuts effect.The distortion is essentially due to transverse

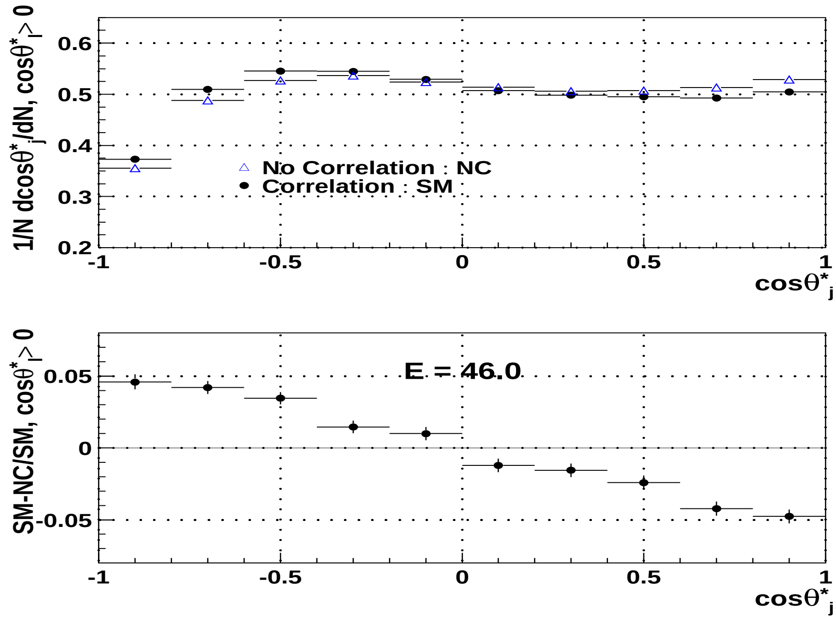

Figure 15: *Distribution of* $\cos\theta_j^*$ *in top or anti-top rest frame for the two models (SM and NC) and fractional difference between the 2 models when* $\cos\theta_\ell^* > 0$ *at the generation level without ISR, FSR and without background with cut on* η *and* p^T *(set 1).*

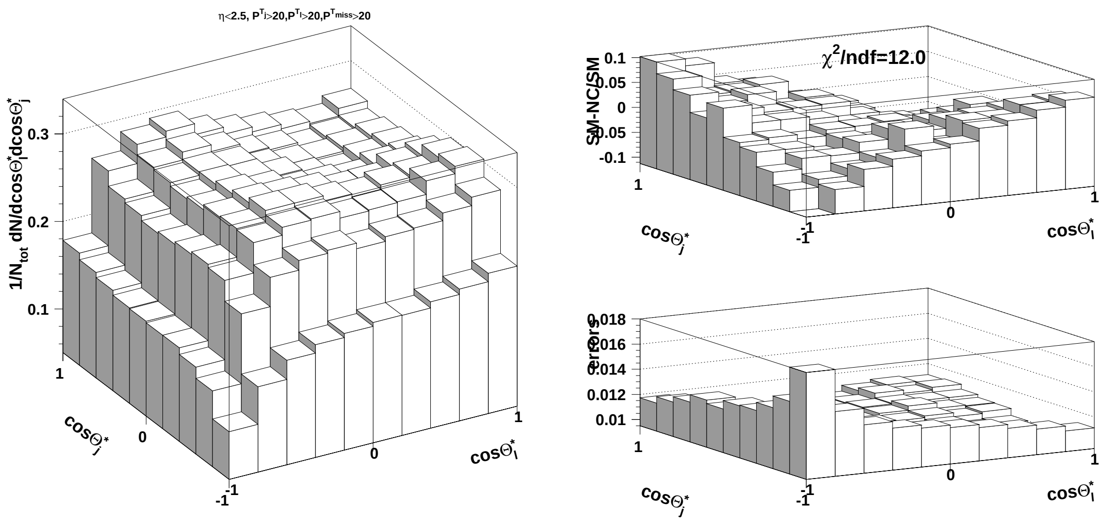

Figure 16: *Distribution of* $\cos\theta_j^*$ *versus* $\cos\theta_\ell^*$ *in top (anti-top) rest frame in Standard Model case (left) and fractionnal difference between the two models (SM and NC) and statistical error (right) at the generation level without ISR, FSR and without background with cut on* η *and* p^T *(set 1).*

momentum cuts. Cuts affect equally the two distributions. At first order, i.e. as in the "no cut" case, the fractionnal difference can be fitted by the followed function :

$$g_{(SM-NC)/SM}(\cos\theta^*_{jet}) = \frac{\alpha_{SM}\cos\theta^*_{jet}}{1+\alpha_{SM}\cos\theta^*_{jet}} \tag{17}$$

Using Figure 15, α_{SM} extracted by the fit is -0.0557 ± 0.0026, which is compatible with the expected value. This approximation became worst when p^T cuts increase. But, the fractionnal difference keeps correlation information with a greater amplitude (5%) than for the laboratory angular distribution given in Figure 7 (1.5%).

Figures 16 left and right show the 3-D plot of the angular distribution given in equation 14 for SM case and the fractionnal difference SM-NC/SM. The first plot is the same as in Figure 4c with set 1 cuts applied. As in Figure 16, the curve is distorted, but the fractionnal difference is not much affected.

To extract the decay particles 4-momentum in the top rest frame, a good jet recalibration is required to compute the neutrino longitudinal momentum without introduction of additionnal errors (pricipally due to ISR and FSR) and to reconstruct the top 4-momentum. A low level of bad b-qq jets/b-$\ell\nu$ association is also necessary to reconstruct top or anti-top rest frame. Therefore, efficient association criteria has to be found. Examples of such criteria are described in [20] where an association criteria efficiency of 69% with a purity of 68% is reached.

With optimized t and $\bar{t}$ reconstruction, spin correlation parameters α and κ can be measured out of $t\bar{t}$ decay product angular distributions in the t and $bart$ rest frames.

7 Signature of new physics

Top decay products angular distribution can reveal signature of new physics.

Technicolor models predict $t\bar{t}$ pairs production via the techni-eta η_T resonance [21]. Such resonance increases spin correlation effect in producing same helicities $t\bar{t}$ pairs [11]. The effect depends on branching ratio of the η_T decaying in $t\bar{t}$ pairs. Using the minimal cross section for a η_T discovery at the LHC after one year at low luminosity [22], i.e. 17 pb for a 400 GeV/c^2 η_T mass, one find a 3.3% increase of asymmetry, leading to maximal deviations of half percent in the Figure 4**c** angular distribution.

Top quark decay in a supersymmetric charged Higgs boson and a b quark can change spin correlation parameters [11]. In that case, α values in $t \to Hb \to bjj$ are $\alpha_b = 1.0$ and $\alpha_j = (\xi^2+1+2\ln\xi)/(\xi-1)^2$, where $\xi = m_t^2/m_H^2$. A two jets of Higgs decay is suppressed compared to the $\tau\nu_\tau$ leptonic decay [23]. Nevertheless, for a $M_{H^+} < 150$ GeV/c^2 and for a small $\tan\beta$, the decay in two jets is not negligeable. With $M_{H^+} = 130$ GeV/c^2 and $\tan\beta = 1.5$ [24], a 0.1% maximum deviation is expected in Figure 4**c** angular distribution. Moreover the deviation is increased up to 0.3% in the angular distribution of lepton and b quark for an ideal reconstruction case.

As already said, a CP violation in Higgs sector [7, 13] can affect spin correlation predicted by Standard Model. Figure 17 shows first order Feynman graphs with this CP violation.

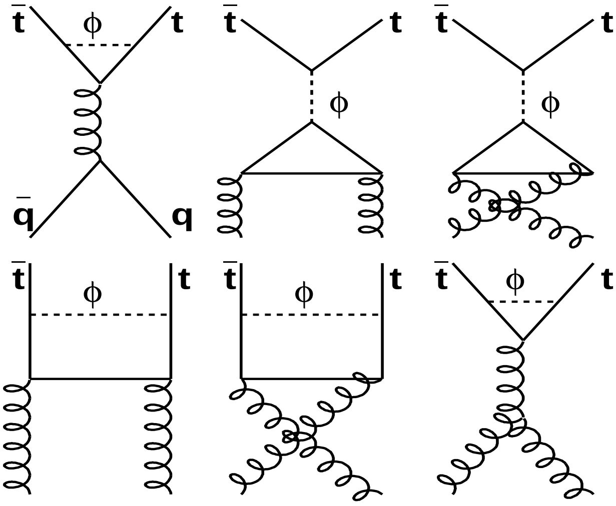

Figure 17: *Feynman graphs which produce CP violation in the processes $q\bar{q} \to t\bar{t}$ and $gg \to t\bar{t}$.*

Exchange of ϕ Higgs boson induces CP-violating final-state interactions in $t\bar{t}$ production. This modifies the number of left helicity pairs with respect to right helicity pairs. This asymmetry, called ζ, is defined as :

$$\zeta = \frac{N_{LL} - N_{RR}}{N_{tot}} \tag{18}$$

where N_{LL} (N_{RR}) is the left (right) helicity pairs number and N_{tot} the total number of $t\bar{t}$ pairs. The proportions of t_L and t_R are respectively $(1+\zeta)/2$ and $(1-\zeta)/2$. Equations 10, 11, 12 and 13 become respectively :

$$P^R_{\ell^+}(y) = \frac{(1-\zeta)\left(2+\alpha^R_{\ell^+}(1+y)\right)}{4+2\zeta\alpha^R_{\ell^+}(1+y)}\ , \tag{19}$$

$$P_{\bar{t}_R} = \frac{A-\zeta^2}{1-\zeta^2}P_{t_R} + \frac{1-A}{2(1+\zeta)} \tag{20}$$

$$P_{\bar{t}_L} = \frac{-A+\zeta^2}{1-\zeta^2}P_{t_R} + \frac{A+1+2\zeta}{2(1+\zeta)} \quad \text{and} \tag{21}$$

$$\frac{1}{N_{tot}}\frac{dN}{d\cos\bar{\theta}^*_j} = \frac{1}{2}\left(1+\bar{\alpha}^L_j\left(\frac{A+\zeta}{1+\zeta} - \frac{2(A-\zeta^2)}{1-\zeta^2}P_{t_R}\right)\cos\bar{\theta}^*_j\right) \tag{22}$$

Expected values of ζ are in order of 10^{-3}. With $\zeta = 0.005$, a 0.2% deviation is observed in Figure 15 angular distribution.

A test of the weak curent structure in tbW vertex is also possible. A small contribution of the V+A structure in the tbW vertex , vertex parametrized by $g_V\gamma^\mu + g_A\gamma^\mu\gamma^5$, affects alpha values [14]. g_V and g_A can be written as :

$$g_V = \frac{1+\delta}{\sqrt{1+\delta^2}} \text{ and } g_A = \frac{-1+\delta}{\sqrt{1+\delta^2}},$$

with $\delta = 0$ in the Standard Model case corresponding to a pure V–A structure. In the general case, α for the charged lepton and for the neutrino are :

$$\alpha_\ell = 1 - \frac{\delta^2}{1+\delta^2}h(u) \tag{23}$$

$$\alpha_\nu = -\Big(1-h(u)\Big)\Big(1+\frac{\delta^2}{1+\delta^2}\frac{h(u)}{1-h(u)}\Big) \tag{24}$$

where

$$h(u) = 2 - \frac{12u(1-u+u\ln u)}{(1-u)^2(1+2u)},\ u = M_W^2/m_t^2 \tag{25}$$

A δ value of 0.1 leads to α coefficients of 0.993 and -0.333 respectively for charged lepton and neutrino. The effect on angular distributions will be, as for the other models, below the percent.

8 Conclusion

Because of the high statistics of the semileptonic channel $t\bar{t} \to WbWb \to \ell\nu bjjb$ and despite initial and final radiation, high background level and a small κ, the $t\bar{t}$ spin correlation effect can be measured by the ATLAS experiments. After three years at low luminosity, the 2σ sensitivity to distinguish between models is 0.8%. This study was done with a fast detector simulation and gives a rough estimate of this sensitivity.

Signature of new physics is expected to affect top decay products angular distributions below the percent. The sensitivity in semileptonic channel seems to be limited to measure a deviation greater than 2σ. But, combined with the complementary dileptonic channel, the sensitivity of measurement should increase.

Other variables can be used to improve sensitivity, such as lepton transverse energy in laboratory frame or $(\vec{p}_b - \vec{p}_{\bar{b}}) \cdot (\vec{p}_\ell \wedge \vec{p}_{jet})$ where $\vec{p}_b$, $\vec{p}_{\bar{b}}$, $\vec{p}_\ell$, $\vec{p}_{jet}$ are the momenta of b, $\bar{b}$, lepton and jet in the laboratory frame [13]. The angular distribution between lepton and b quark can also be considered, particularly to search for a charged Higgs decay into bjj.

However, in order to better quantify the new physics effects, it is necessary to completely simulated these models.

Furthemore, one neutrino final state in semileptonic channel allows to calculate the particle direction in the top rest frame. Thus, a direct α and κ measurements are possible.

Waiting for the LHC, the Tevatron is the unique collider capable to allow $t\bar{t}$ spin correlation measurement. The D0 experiment used a set of six events in the dileptonic channel for a 125 pb^{-1} integrated luminosity (Run1) and a 1.8 TeV center of mass energy

[25]. The experiment estimated the κ value comparing data to simulation with a likelihood function and obtained κ greater than -0.25 with 68% confidence level, in agreement with the Standard Model which predict $\kappa = 0.88$ for the Tevatron. The CDF experiment measured the W helicity in $t\bar{t}$ decay [26]. The fraction of longitudinal W (P_{W_L}) from all Wb top decays is $P_{W_L} = m_t^2/(m_t^2 + 2M_W^2) = 70\%$. P_{W_L} and α_W are connected as $P_{W_L} = (1 + \alpha_W)/2$. With a 106 pb^{-1} integrated luminosity, CDF measured P_{W_L} from 108 $t\bar{t}$ pairs (semileptonic and dileptonic channel) studying the transverse impulsion of charged lepton. A value of $0.91 \pm 0.37 \pm 0.13$ was obtained, in agreement with Standard Model predictions.

With a 2 fb^{-1}/year integrated luminosity during Run2 phase, 30 fb^{-1}/year during Run3, and with a 2 TeV center of mass energy, CDF and D0 experiments will increase their $t\bar{t}$ pair samples allowing more precise $t\bar{t}$ spin correlation measurements. The advantage, compared to the LHC, is to have a higher κ value, because the energy spectrum is not the same as at LHC. But the number of $t\bar{t}$ pairs produced at Run2 ($\sim$ 16 000) can be statistically insufficient to measure signature of new physics through $t\bar{t}$ spin correlations.

The ATLAS experiment, with lower κ but higher statistics, will complete the Tevatron $t\bar{t}$ spin correlation research and will be able to identify new physics phenomena in $t\bar{t}$ spin correlation studies with a sensitivity below the percent.

References

[1] F. Abe et al., *Observation of Top Quark Production in p-barp Collisions with the Collider Detector at Fermilab*, Phys. Rev. Lett. 74, 2626 (1995).

[2] S. Abachi et al., *Observation of the Top Quark*, Phys. Rev. Lett. 74, 2632 (1995).

[3] D.E.Groom et al., *Review of Particle Physics*, The European Physical Journal C15 (2000), p.385-387.

[4] L.H.Orr, *Decay versus hadronization for top quarks produced in hadron colliders*, Phys. Rev. D44, 88 (1991).

[5] V.Barger, J.Ohnemus, R.J.N. Phillips, *Spin correlation effects in the hadroproduction and decay of very heavy top quark pairs*, Int. Journal of Modern Physics A, Vol. 4, No 3 (1989), 617-625.

[6] I.Bigi, Y.Dokshitzer,V.Khoze,J.Kühn and P.Zerwas, *Production and decay properties of ultra-heavy quarks*, Phys. Lett. B181, 157 (1986).

[7] S.Weinberg, *Larger Higgs-Bosons-Exchange Terms in the Neutron Electric Dipole Moment*, Phys. Rev. Lett. 63, 2333 (1989); S.Weinberg,*Unitarity constraint on CP nonconservation in Higgs-boson exchange*, Phys. Rev. D42, 860 (1990).

[8] V.Simak, J.Smolik, A.Lagatta, *Measurement of Top-Antitop Spin Correlations in the ATLAS Experiment*, ATL-PHYS-2000-032.

[9] R.Bonciani, S.Catani, M.L.Mangano, P.Nason, *NLL resummation of the heavy-quark hadro-production cross-section*, Nucl. Phys. B529 (1998) 424.

[10] A.P.Heinson, *Future top physics at the Tevatron and LHC*, D0 note 2961 UCR/D0/97-17, FERMILAB conf-96-116-E.

[11] G.Mahlon, S.Parke, *Angular correlations in top quark pair production and decay at hadron collider*, Phys. Rev. D53, 4886 (1996).

[12] N.Cabibbo, Phys. Rev. Lett. 10, 531 (1963); M.Kobayashi, T.Maskawa, Prog. Theor. Phys. 49, 652 (1973).

[13] G.L. Kane, G.A. Ladinsky, C.P. Yuan, Phys. Rev. D45, 124 (1992); C.R.Schmidt, M.Peskin, Phys. Rev. Lett. 69, 410 (1992); W.Bernreuther, A.Brandenburg, Phys. Lett. B314, 104 (1993); W. Bernreuther, A.Brandenburg, Phys. Rev D49, 4481 (1994).

[14] M.Jeżabek, J.H.Kühn, *V-A test through leptons from polarised top quarks*, Phys. Lett. B329, 317 (1994).

[15] ATLAS Collaboration, *Detector and Physics performance Technical Design Report*, CERN/LHCC/99-15, p.619-645.

[16] T.Sjöstrand, *PYTHIA 5.7 and JETSET 7.4 : Physics and Manual*, LU TP 95-20.

[17] E.Richter-Was, D.Froidevaux and L.Poggioli, *ATLFAST 2.0 a fast simulation package for ATLAS*, ATL-PHYS-98-131.

[18] ATLAS Collaboration, *Detector and Physics performance Technical Design Report*, CERN/LHCC/99-15, p.621.

[19] D.E.Groom et al., *Review of Particle Physics*, The European Physical Journal C15 (2000), p.21.

[20] P.Gernier,D.Pallin,P.Rosnet,L.P.Says, *Measurement of top quark mass in the inclusive lepton jets channel*, ATL-PHYS-99-026.

[21] E.Eichten, K.Lane, *Multiscale technicolor and top production*, Phys. Lett. B327, 129 (1994).

[22] G.Azuelos, P.Depommier, R.Mazini, K.Strahl, *Search for Technicolor Signals with the ATLAS Detector*, ATL-PHYS-99-020.

[23] M. Guchait, D.P.Roy, *Constraints on the charged Higgs sector from the Fermilab Tevatron collider data*, Phys. Rev. D55, 7263 (1997).

[24] ATLAS Collaboration, *Detector and Physics performance Technical Design Report*, CERN/LHCC/99-15, p.769.

[25] B.Abbott et Al., Spin Correlation un $t\bar{t}$ Production from $p\bar{p}$ Collision at $\sqrt{s} = 1.8$ TeV, Phys. Rev. Lett. 85, 256 (2000)

[26] T.Affolder et al., *Measurement of the Helicity of W Bosons in Top Quark Decays*, Phys. Rev. Lett. 84, 216 (2000)